

Reduction in efficiency droop, forward voltage, ideality factor, and wavelength shift in polarization-matched GaInN/GaN multi-quantum-well light-emitting diodes

Jiuru Xu,¹ Martin F. Schubert,¹ Ahmed N. Noemaun,¹ Di Zhu,¹ Jong Kyu Kim,¹ E. Fred Schubert,^{1,a)} Min Ho Kim,² Hun Jae Chung,³ Sukho Yoon,³ Cheolsoo Sone,³ and Yongjo Park³

¹Department of Physics, Applied Physics, and Astronomy, Department of Electrical, Computer, and System Engineering, and Future Chips Constellation, Rensselaer Polytechnic Institute, Troy, New York 12180, USA

²Future Chips Constellation, Rensselaer Polytechnic Institute, Troy, New York 12180, USA and Central R&D Institute, Samsung Electro-Mechanics, Suwon 443-743, Republic of Korea

³Central R&D Institute, Samsung Electro-Mechanics, Suwon 443-743, Republic of Korea

(Received 25 October 2008; accepted 8 December 2008; published online 9 January 2009)

Blue light-emitting diodes (LEDs) with polarization-matched GaInN/GaN multi-quantum-well (MQW) active regions are grown by metal-organic vapor-phase epitaxy. The GaInN/GaN MQW structure reduces the magnitude of polarization sheet charges at heterointerfaces in the active region. The GaInN/GaN MQW LEDs are shown to have enhanced light-output power, reduced efficiency droop, a lower forward voltage, a smaller diode ideality factor, and decreased wavelength shift, compared with conventional GaInN/GaN MQW LEDs. © 2009 American Institute of Physics. [DOI: 10.1063/1.3058687]

A major obstacle for GaInN based light-emitting diodes (LEDs) to further penetrate into the general illumination market is that their efficiency suffers a substantial decrease as the injection current increases; this well-known phenomenon is called “efficiency droop.” The efficiency of conventional GaInN/GaN multi-quantum-well (MQW) LEDs generally reaches its peak value at forward current densities less than 10 A/cm² and monotonically drops as the current increases further.¹ The efficiency droop is caused by a nonradiative carrier loss mechanism that becomes dominant as the injection current increases.² Its physical origin remains under discussion. Electron leakage,¹⁻³ lack of hole injection,⁴⁻⁷ carrier delocalization,^{8,9} Auger recombination,^{10,11} defects,¹² and junction heating¹³ were suggested as explanations.

Both electron leakage and lack of hole injection result in an electron current that crosses the electron-blocking layer (EBL). These electrons then recombine with holes outside the active region. Although these two mechanisms (electron leakage and lack of hole injection) are usually both described by the term “carrier leakage,” they lead to distinctly different proposals as to reduce the efficiency droop. Leaking electrons from the active region indicates that the conventional conduction-band design is not adequate to prevent electrons from entering the *p*-side of the device;¹⁻³ novel conduction-band engineering could result in better electron confinement. On the other hand, lack of hole injection indicates that the valence-band and acceptor-doping design is not adequate to introduce a sufficient number of holes into the active region. Accordingly, a *p*-type active region design was proposed to facilitate hole injection.^{6,7}

One proposed approach to minimize the electron leakage current from the active region is to reduce the contrast in material polarization.¹ It is well known that the polarization mismatch, which occurs at heterointerfaces results in the for-

mation of large sheet charges, which modify the bands to form large triangular barriers in the MQW active region and the EBL. These barriers create obstacles for carriers and require high forward voltages for significant currents to flow, so that the conduction band on the *n*-side of the device is significantly higher than the conduction band on the *p*-side. This makes it energetically favorable for electrons to escape to the *p*-side of the device. This is elucidated in Fig. 1(a), which shows the simulated conduction band diagram of a

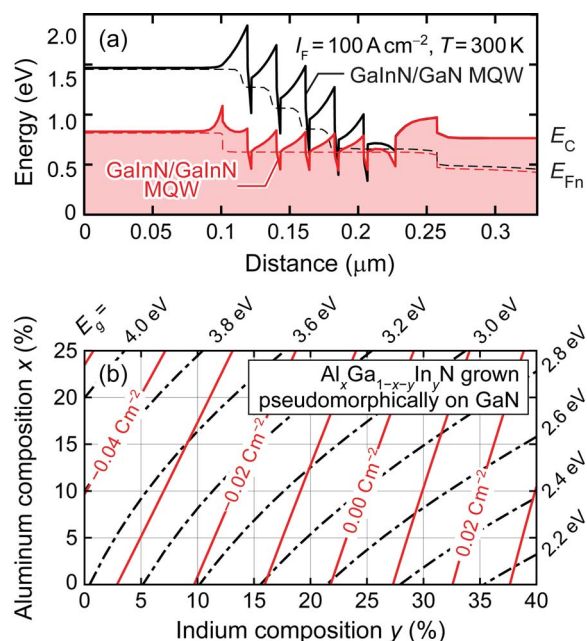


FIG. 1. (Color online) (a) Simulated conduction band diagram of GaInN/GaN and reference GaInN/GaN MQW LEDs at a 100 A/cm² forward current density. (b) Ga-face polarization field charge (red line) and bandgap contours (dashed line) of quaternary Al_xGa_{1-x-y}In_yN grown pseudomorphically on GaN substrates.

^{a)}Electronic mail: efschubert@rpi.edu.

GaNN/GaN MQW LED with reduced polarization mismatch in comparison with the conventional GaInN/GaN MQW LED at the forward current density of 100 A/cm^2 . The GaInN/GaN MQW structure has much lower triangular barriers in the active region. The conduction band on the n -side of the device is approximately the same height as the conduction band on the p -side, which indicates that the polarization-matched active region design minimizes the driving force for electrons to leak out of the active region, as proposed above. At the same forward current density the GaInN/GaN MQW design has reduced electron leakage from active region as evidenced by the greater separation of the electron quasi-Fermi level from the conduction band edge in the p -type region as compared to the reference GaInN/GaN MQW structure [see Fig. 1(a)]. Figure 1(b) gives the bandgap and material polarization of quaternary alloy $\text{Al}_x\text{Ga}_{1-x-y}\text{In}_y\text{N}$ pseudomorphically grown on GaN as a function of the Al and In compositions. By appropriate selection of the barrier composition, good electron confinement and reduction in the polarization mismatch can be achieved. In this work, we present a GaInN/GaN MQW design with reduced polarization mismatch that maintains the Al-free characteristic of conventional GaInN/GaN MQW active region.

The structures are grown on c -plane sapphire by metal-organic vapor-phase epitaxy. After ten minutes pretreatment of the substrate in H_2 and NH_3 ambient at 1100°C , a 500°C low-temperature GaN buffer is deposited. A $2 \mu\text{m}$ thick unintentionally doped GaN is grown at 1100°C , followed by $3 \mu\text{m}$ thick Si-doped n -type GaN layer grown at 1010°C . A five period GaInN/GaN MQW active region is grown, followed by a p -type $\text{Al}_{0.13}\text{Ga}_{0.87}\text{N}:\text{Mg}$ EBL and a p -type GaN cladding layer. In addition, a reference LED with conventional GaInN/GaN MQW active region is grown with otherwise the same structure as the GaInN/GaN MQW devices. The central electroluminescence wavelength is near 440 nm for both the GaInN/GaN MQW and GaInN/GaN MQW sample. Wafers are processed into $1 \times 1 \text{ mm}^2$ lateral-structure devices and the sapphire substrate is thinned for dicing.

Unencapsulated devices are tested in pulsed mode with 500 Hz frequency and 1% duty cycle to prevent self-heating effects. The tests are done at room temperature with forward current up to 3 A . Three randomly chosen devices are tested for each of the GaInN/GaN MQW and reference GaInN/GaN MQW samples. Almost identical characteristics are obtained for each type of device. Figure 2(a) shows the normalized light-output power as a function of forward current density for both GaInN/GaN MQW LEDs and the reference GaInN/GaN MQW LEDs. Figure 2(b) shows the normalized external quantum efficiency (EQE) of these two types of devices. The EQE of the reference GaInN/GaN MQW LED reaches its peak at very low current density, 4 A/cm^2 , and decays rapidly as the forward current density increases. At 300 A/cm^2 , the EQE of the reference GaInN/GaN MQW LEDs drops below 50% of its peak value. In comparison, the GaInN/GaN MQW LEDs reach the EQE peak at higher current density, 22 A/cm^2 , and outperform the reference GaInN/GaN MQW LEDs when the forward current density increases beyond 34 A/cm^2 . The EQE peak ratio between GaInN/GaN and reference GaInN/GaN MQW LEDs is 84% , which is higher than for the GaInN/AlGaIn MQW approach.³ The increase in the low-current

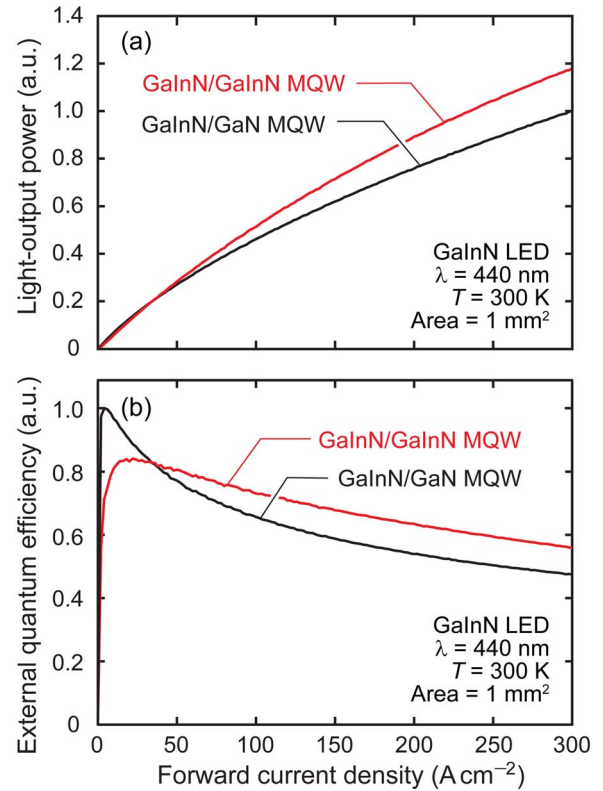


FIG. 2. (Color online) (a) Normalized light-output power as a function of forward current density for GaInN/GaN and reference GaInN/GaN MQW LEDs. (b) Normalized external quantum efficiency as a function of forward current density for GaInN/GaN and reference GaInN/GaN MQW LEDs.

peak efficiency shows longer nonradiative lifetime and potentially better crystal quality of the GaInN/GaN MQW LEDs, which we attribute to the Al-free active region. At the maximum forward current density of 300 A/cm^2 , an 18% increase in the light-output power is achieved by implementing the GaInN/GaN MQW structure.

Figure 3 shows the electrical characteristics of the two

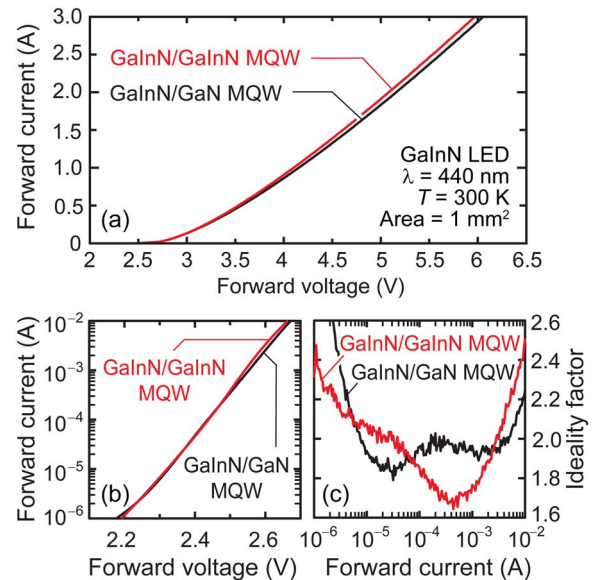


FIG. 3. (Color online) Electrical characteristics comparison between the GaInN/GaN and reference GaInN/GaN MQW LEDs: (a) forward current as a function of voltage, (b) low-current IV characteristics, and (c) ideality factor comparison.

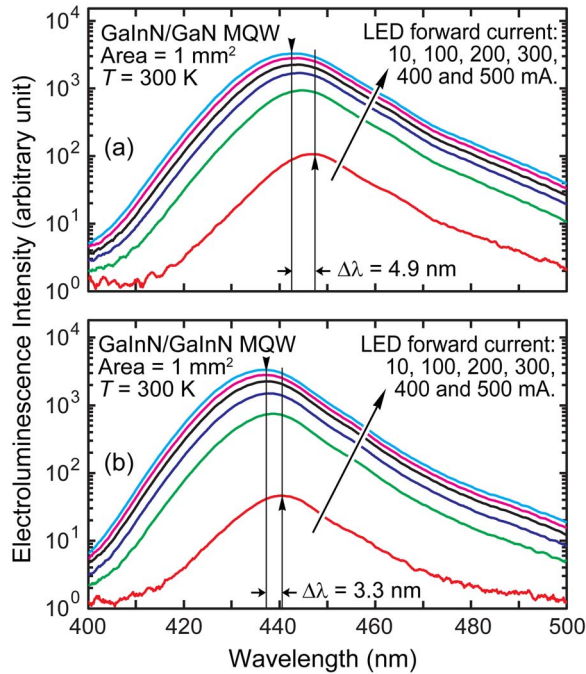


FIG. 4. (Color online) Electroluminescence spectra at various injection currents with peak wavelength shift indicated: (a) reference GaInN/GaN MQW LEDs and (b) GaInN/GaN MQW LEDs.

types of devices. The GaInN/GaN MQW LEDs have lower forward voltage compared with the reference GaInN/GaN MQW LEDs as shown in Fig. 3(a); this is consistent with the simulation results shown in Fig. 1(a). The reduction in forward voltage further increases the wall-plug efficiency of the GaInN/GaN MQW LEDs to 22% compared to the reference GaInN/GaN MQW LEDs. Figure 3(b) shows the 1 μ A to 10 mA current-voltage (IV) comparison in a semilogarithm plot. No subthreshold turn-on is observed and the forward voltage at 1 μ A is approximately 2.2 V for both samples, which indicates that the GaInN/GaN MQW approach maintains good crystal quality while enhancing the light-output power and reducing the efficiency droop. Figure 3(c) compares the ideality factor of the GaInN/GaN MQW LEDs with the reference GaInN/GaN MQW LEDs. The ideality factor at intermediate currents gives insight into the IV characteristics of the junction itself, since series resistance dominates the IV relation at high forward current and shunt resistance dominates at very low forward current.¹⁴ The ideality factor is below 1.7 for GaInN/GaN MQW LEDs and around 2.0 for the reference GaInN/GaN MQW LEDs in the intermediate current range. Finally, the GaInN/GaN MQW LEDs have also reduced electroluminescence wavelength shift with increasing forward current. The emission spectra of the two types of devices at various current levels are as

shown in Fig. 4; the peak wavelength shift ($\Delta\lambda$) is reduced from 4.9 nm for the reference GaInN/GaN MQW LED sample to 3.3 nm for the GaInN/GaN MQW LED sample as the forward current changes from 10 to 500 mA. The reduction in $\Delta\lambda$ is consistent with the reduction in the electric field in the quantum wells and the associated quantum-confined Stark effect.

In summary, we have demonstrated polarization-matched GaInN/GaN MQW LEDs with strongly improved optical and electrical properties. Compared with conventional GaInN/GaN MQW LEDs, the GaInN/GaN MQW LEDs show an 18% increase in light-output power, a 22% increase in wall-plug efficiency, a reduction in efficiency droop, forward voltage, diode ideality factor, wavelength shift, and no subthreshold turn on. Based on theoretical simulations, these improvements are consistent with the concept of polarization matching and reduced electron leakage.

The authors gratefully acknowledge support by Samsung Electro-Mechanics Co., National Science Foundation, Smart Lighting Engineering Research Center, Sandia National Laboratories, Rochester Institute of Technology, Department of Energy, Department of Defense, Magnolia Optics, Crystal IS, Troy Research Corporation, and New York State.

- ¹M. H. Kim, M. F. Schubert, Q. Dai, J. K. Kim, E. F. Schubert, J. Piprek, and Y. Park, *Appl. Phys. Lett.* **91**, 183507 (2007).
- ²M. F. Schubert, S. Chhajed, J. K. Kim, E. F. Schubert, D. D. Koleske, M. H. Crawford, S. R. Lee, A. J. Fischer, G. Thaler, and M. A. Banas, *Appl. Phys. Lett.* **91**, 231114 (2007).
- ³M. F. Schubert, J. Xu, J. K. Kim, E. F. Schubert, M. H. Kim, S. Yoon, S. M. Lee, C. Sone, T. Sakong, and Y. Park, *Appl. Phys. Lett.* **93**, 041102 (2008).
- ⁴T. A. Pope, P. M. Smowton, P. Blood, J. D. Thomson, M. J. Kappers, and C. J. Humphreys, *Appl. Phys. Lett.* **82**, 2755 (2003).
- ⁵J. Xie, X. Ni, Q. Fan, R. Shimada, U. Ozgur, and H. Morkoc, *Appl. Phys. Lett.* **93**, 121107 (2008).
- ⁶I. V. Rozhansky and D. A. Zakheim, *Phys. Status Solidi C* **3**, 2160 (2006).
- ⁷I. V. Rozhansky and D. A. Zakheim, *Phys. Status Solidi A* **204**, 227 (2007).
- ⁸A. Y. Kim, W. Götz, D. A. Steigerwald, J. J. Wierer, N. F. Gardner, J. Sun, S. A. Stockman, P. S. Martin, M. R. Krames, R. S. Kern, and F. M. Steranka, *Phys. Status Solidi A* **188**, 15 (2001).
- ⁹S. F. Chichibu, T. Azuhata, M. Sugiyama, T. Kitamura, Y. Ishida, H. Okumura, H. Nakanishi, T. Sota, and T. Mukai, *J. Vac. Sci. Technol. B* **19**, 2177 (2001).
- ¹⁰Y. C. Shen, G. O. Müller, S. Watanabe, N. F. Gardner, A. Munkholm, and M. R. Krames, *Appl. Phys. Lett.* **91**, 141101 (2007).
- ¹¹N. F. Gardner, G. O. Müller, Y. C. Shen, G. Chen, S. Watanabe, W. Götz, and M. R. Krames, *Appl. Phys. Lett.* **91**, 243506 (2007).
- ¹²B. Monemar and E. B. Sernelius, *Appl. Phys. Lett.* **91**, 181103 (2007).
- ¹³A. A. Efremov, N. I. Bochkareva, R. I. Gorbunov, D. A. Larinovich, Yu. T. Rebane, D. V. Tarkhin, and Yu. G. Shreter, *Semiconductors* **40**, 605 (2006).
- ¹⁴E. F. Schubert, *Light-Emitting Diodes*, 2nd ed. (Cambridge University Press, Cambridge, 2006), Chap. 4.